Pure Appl. Chem., Vol. 84, No. 8, pp. 1713–1727, 2012.
http://dx.doi.org/10.1351/PAC-CON-11-12-06

Pd/TOMPP-catalyzed telomerization of 1,3-butadiene: From biomass-based substrates to new mechanistic insights*

Peter J. C. Hausoul[1,2], Pieter C. A. Bruijnincx[2], Bert M. Weckhuysen[2], and Robert J. M. Klein Gebbink[1,‡]

[1]*Organic Chemistry and Catalysis, Debye Institute for Nanomaterials Science, Utrecht University, Universiteitsweg 99, 3584 CG, Utrecht, The Netherlands;*
[2]*Inorganic Chemistry and Catalysis, Debye Institute for Nanomaterials Science, Utrecht University, Universiteitsweg 99,*
3584 CG, Utrecht, The Netherlands

Abstract: Studies aimed at synthesizing surfactants from biomass-based feedstocks using Pd-catalyzed telomerization of 1,3-butadiene resulted in the development of a highly active catalyst system. A ligand screening was performed, and Pd/tris(2-methoxyphenyl)phosphine (TOMPP) was identified as the most promising catalyst. A solvent- and base-free protocol was developed, which allows efficient and selective conversion of a wide variety of polyol substrates (e.g., glycerol, diols, carbohydrates, and sugar alcohols). In the case of hemi-acetal bearing sugars, catalyst deactivation was observed and mechanistic studies showed that extensive formation of ligand-derived phosphonium species depleted the amount of available ligand. Stoichiometric coordination reactions gave insight into the phosphine alkylation mechanism and demonstrated the reversibility of the observed reaction. A simple and efficient one-pot synthesis method was developed for the preparation of $[Pd((1\text{-}3,7,8\eta)\text{-}(E)\text{-octa-}2,7\text{-dien-}1\text{-yl})(PR_3)]^+$ complexes, which are key reactive intermediates. Based on these studies, an extended telomerization mechanism is proposed, which accounts for the formation of ligand-derived phosphonium species and the reversibility of reaction pathways.

Keywords: biomass; palladium catalysis; telomerization.

INTRODUCTION

Over recent decades, it has become clear that diminishing fossil fuel reserves and a growing global population are necessitating a shift from the current oil-based society toward a more sustainable renewables-based society. In terms of chemical production, this has spurred the exploration of numerous catalytic processes in combination with biomass-based feedstocks for the sustainable production of fuels and chemicals [1,2]. Owing to the highly oxygenated, multifunctional nature of biomass-based chemicals (e.g., glycols, glycerol, sugars, etc.) these often polar molecules constitute very suitable starting materials for the production of, e.g., surfactants. In this regard, alkylation reactions such as the acid-catalyzed etherification of alkenes [3] and the Pd-catalyzed telomerization of 1,3-butadiene [4] constitute

---

Pure Appl. Chem.* **84, 1673–1784 (2012). A collection of invited papers based on presentations at the 16th International Symposium on Organometallic Chemistry Directed Towards Organic Synthesis (OMCOS-16), Shanghai, China, 24–28 July 2011.

‡Corresponding author

attractive and efficient routes for the valorization of biomass-based feedstocks. As shown in Scheme 1, both reactions are, in principle, 100 % atom-efficient. In the case of etherification, a branched octyl ether (main product) and minor amounts of the linear octyl ether are directly obtained, whereas for Pd-catalyzed telomerization, linear (main product) and branched octadienyl ethers are obtained which require an additional hydrogenation step to yield the respective saturated octyl ethers.

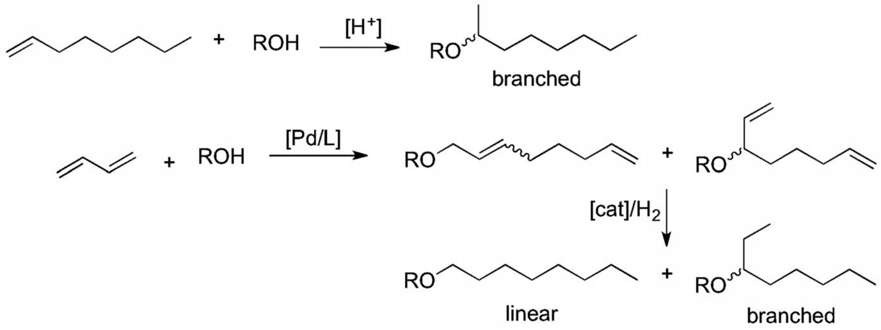

Scheme 1 Overall reactions of the acid-catalyzed etherification of alcohols with 1-octene and the Pd-catalyzed telomerization of 1,3-butadiene with alcohols followed by hydrogenation.

We have recently studied both routes in combination with biomass-based alcohols [5,6]. For the etherification reaction good conversions and high selectivities toward the desired ether products were obtained using H-beta zeolite catalysts, however, the inherently biphasic nature of the reaction mixture and deactivation processes greatly limit the scope of the alcohols and olefins that can be employed [5b]. A detailed comparison of the advantages and disadvantages of the two routes has recently been published by Parvulescu et al. [7]. Here, we present an overview of the results obtained for the Pd/tris(2-methoxyphenyl)phosphine (TOMPP)-catalyzed telomerization of 1,3-butadiene with biomass-based substrates and the insights into these reactions obtained from supporting mechanistic studies [6,8].

RESULTS AND DISCUSSION

The Pd-catalyzed telomerization of 1,3-butadiene is a highly useful synthetic reaction that is commercially applied for the production of 1-octanol (i.e., via Pd-catalyzed telomerization of water followed by hydrogenation) [9] and 1-octene (i.e., via Pd-catalyzed telomerization of methanol followed by hydrogenation and elimination of methanol) [10]. Over the years, much research has been dedicated to the optimization of process conditions and catalysts, exploration of substrate scope, and mechanistic studies. As a result, the understanding of this catalytic reaction is very well developed and many aspects of this versatile reaction have recently been reviewed [4]; they will not be discussed in detail except where relevant.

Crude glycerol and Pd/TOMPP

The telomerization work in our group has been mainly focused on the production of surfactants from biomass-based feedstocks. One such feedstock is crude glycerol, which is a waste product of the production of biodiesel (constituting 110 kg/ton biodiesel produced). European legislation demands that the market share of biodiesel is steadily increasing over the years, which consequently also leads to much higher production volumes of crude glycerol. Given the relatively limited existing market for glycerol-derived consumer products and its requirement of high-purity glycerol, it is expected that prices for crude glycerol will remain low, making new routes for the valorization of this crude feed very attractive.

As a result, various studies have been initiated that explore the utility of glycerol for the production of bulk chemicals such as solvents, fuel additives, polymer intermediates, and surfactants [11]. In the case of the Pd-catalyzed telomerization of 1,3-butadiene with glycerol (**1**), a number of different products can be obtained (Scheme 2). After a single catalytic reaction, the mono-telomer (**1a/1b**) is obtained. Since all hydroxyl groups are reactive in the telomerization reaction, a second and third reaction can occur on the same substrate resulting in the formation of di- (**1c/1d**) and tri-telomers (**1e**), respectively. Therefore, the optimization of process conditions to obtain pure products is an essential aspect of this research. Behr et al. first studied the telomerization of 1,3-butadiene with glycerol using the Pd/TPPTS (TPPTS: 3,3',3''-phosphinidynetris(benzenesulfonic acid) trisodium salt) catalyst in an aqueous biphasic system, which allowed easy separation of the product and reuse of the water-soluble catalyst [3]. Selectivities of >95 % toward the mono-telomers were obtained, however, continued operation resulted in catalyst deactivation, which was attributed to decomposition of the ligand and metal leaching. Although the production of either pure mono- or di-telomers is clearly preferred, depending on the specific target application, mixtures of mono- and di-telomers may also provide suitable product properties. Therefore, we chose to study the direct conversion of glycerol without the use of solvent or any of the commonly used base additives.

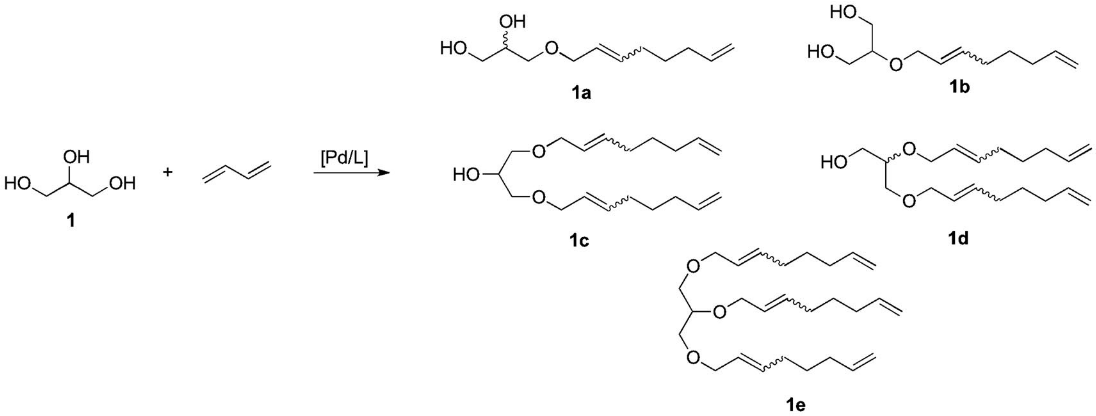

Scheme 2 Pd/L-catalyzed telomerization of 1,3-butadiene with glycerol (branched products not shown for clarity).

Previous studies by Prinz et al. [13] and Estrine et al. [14] regarding the influence of the ligand backbone on catalyst activity had already shown that substitution at the *ortho* positions has a positive effect on product selectivity. A set of *ortho-* and *para*-substituted triphenylphosphine ligands was screened to determine which catalyst was most suited for the conversion of glycerol under these conditions (Fig. 1) [6a]. The screening was performed using a metal-loading of 0.06 mol % Pd(acac)$_2$ (acac: acetylacetonate) with respect to the substrate and with a ligand-to-metal ratio (**P/Pd**) of 5. The butadiene-to-substrate ratio (**Bu/S**) was set at 2.5, and reactions were run at 80 °C for 5 h. In cases where the reaction was fast, the reaction time was reduced to 1 or 0.5 h. The results show that going from **L1** to **L3** particularly the turnover frequency (TOF) increased markedly from 200 h^{-1} for **L1** to 3040 h^{-1} for **L3** (Fig. 2). Also, the combined selectivity toward mono- and di-telomers increased from 72 % for **L1** to 87 % for **L3**. Going on to **L4** and **L5**, the TOF dropped considerably to 499 h^{-1} for **L4** and 50 h^{-1} for **L5**, and in case of **L4** the selectivity was reduced to 71 %. Finally, ligands **L6**, **L7**, and **L8** resulted in much lower conversions and TOFs. From these results, it was concluded that **L3**, TOMPP, is the most active ligand for glycerol telomerization as it presents an optimum between catalyst activity and selec-

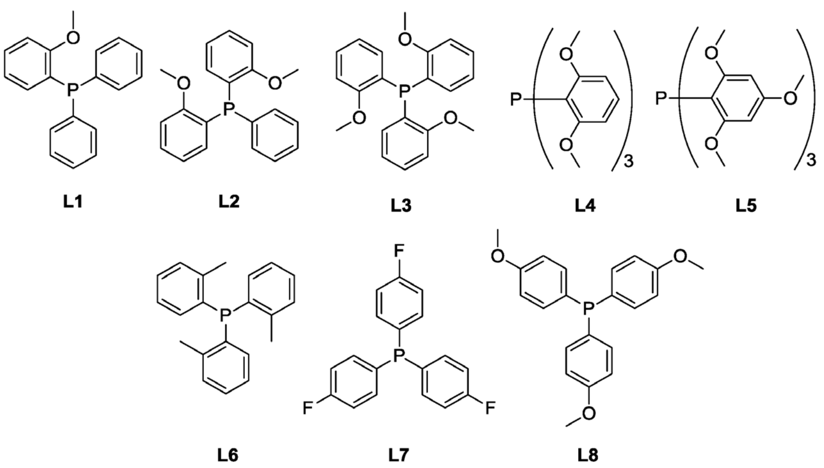

Fig. 1 Ligands used in the solvent- and base-free Pd-catalyzed telomerization of 1,3-butadiene with glycerol [6a].

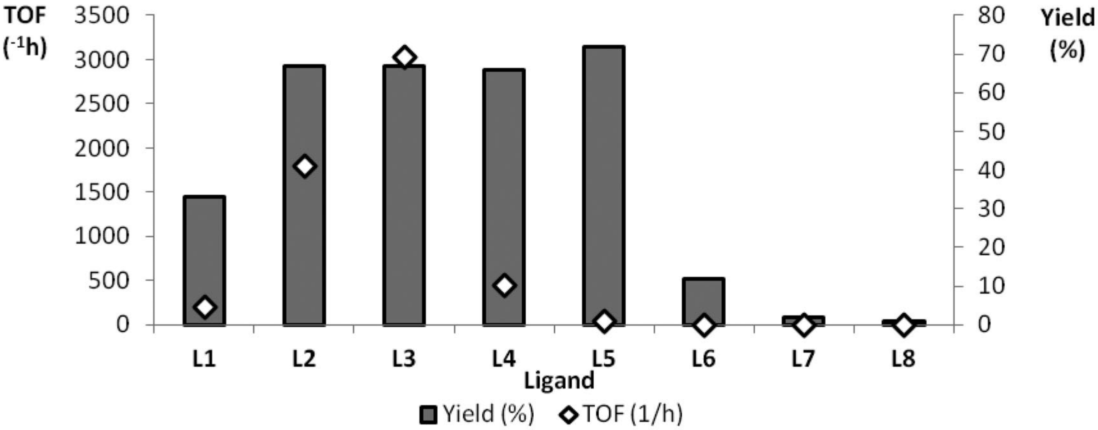

Fig. 2 Activity of different catalysts in the telomerization of 1,3-butadiene with glycerol [6a] (conditions: 0.06 mol % Pd(acac)$_2$, **P/Pd** = 5, **Bu/S** = 2.5, 80 °C).

tivity. Subsequently, the activity of **L3** was also tested in the direct conversion of crude glycerol. Overall, similar activities were observed as for pure glycerol, albeit that selectivities toward mono- and di-telomers were markedly less as a result of the rather high water content. A considerable portion of the water present was also converted to octadienol.

These results demonstrate that Pd/TOMPP is a highly active telomerization catalyst, which allows direct conversion of both pure and crude glycerol without the use of solvents or base additives. Based on these promising results, the Pd/TOMPP catalyst system was further optimized by studying the influence of process parameters such as metal precursor, **P/Pd** ratio, and **Bu/S** ratio [6b]. Variation of the metal precursor showed that Pd(II) salts with halide ligands [e.g., PdCl$_2$ and PdCl$_2$COD (COD: (*Z*,*Z*)-cycloocta-1,5-diene)] are inactive and result in very low conversions. In contrast, Pd(II) salts such as Pd(acac)$_2$ and Pd(OAc)$_2$ (OAc: acetate) or Pd(0) precursors [e.g., Pd(dba)$_2$ (dba: dibenzylideneacetone)] gave the most active catalyst systems. Variation of the **P/Pd** ratio showed that near optimal activity is already achieved at a **P/Pd** ratio of 2. In terms of product selectivity, it was found that a **P/Pd** ratio of 5 gave the best results. The **Bu/S** ratio was varied from 1 to 4 and as expected the substrate conversion increased and the product composition shifted toward the increased formation of di- and tri-telomers. The best mono-telomer selectivities (71–81 %) were obtained when low **Bu/S** ratios (1–2.5) and high reaction temperatures (90–100 °C) were used. The effect of addition of NEt_3 to the reaction mixture was also studied. Besides a faster initiation of the reaction, the addition of NEt_3 had little effect on the activity or selectivity of the catalyst. Recent studies by the groups of Van Leeuwen and Briggs have also demonstrated the favorable influence of *ortho*-methoxy groups on the catalytic activity for the telomerization of 1,3-butadiene with methanol [15].

Diols

Similar to glycerol, the selective telomerization of renewable diols [e.g., ethylene glycol (**2**), propylene glycol (**3**)] offers an attractive opportunity for the production of surfactants. In fact, several patents describe the production and use of ethylene glycol telomers [16]. Diols may be obtained from biomass using several different routes [17]. In the open literature, the telomerization of ethylene glycol has also been studied on several accounts and generally high yields and selectivities toward monotelomers are observed [18]. Behr et al. reported the highest mono-telomer selectivity of 99 %, which was obtained using the Pd/TPPTS catalyst under aqueous biphasic reaction conditions. Using the same system, other glycols, such as 1,3-propanediol (**3**) and 1,4-butanediol (**4**), were found to give both lower conversion and selectivity. Using previously optimized conditions, we set out to expand the substrate scope and study the telomerization performance of Pd/TOMPP with a series of linear and branched diols (Fig. 3) [6c,7]. A Pd loading of 0.01 mol % $Pd(acac)_2$ with a **P/Pd** ratio of 5 was used for all reactions.

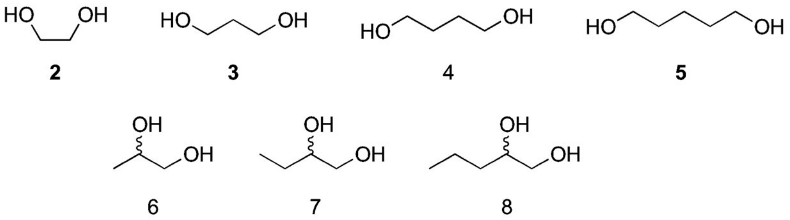

Fig. 3 Linear and branched diols screened in the solvent- and base-free Pd/TOMPP-catalyzed telomerization of 1,3-butadiene [6c,7].

At 80 °C and a **Bu/S** ratio of 2, 76 % of **3** was converted within 27 min. The mono-telomer selectivity under these conditions was 80 %. Under the same conditions, 1,2-propanediol (**6**) was converted by 73 % and displayed a mono-telomer selectivity of 89 %. This shows that the Pd/TOMPP-catalyzed reaction is still quite selective at high conversions. However, when excess amounts of butadiene were used or when the reaction was run for longer periods, the selectivity decreased considerably. For substrates **3–8**, similar selectivities (75–90 %) were observed, whereas for ethylene glycol (**2**) the selectivity was considerably less (53 %). In terms of activity, it was found that the structure of the diol could be correlated to the initial TOF. Short reactions were run for all substrates, and in the case of linear diols the TOF increased from 7206 h^{-1} for **2** to 400000 h^{-1} for **5**. A similar acceleration was also observed for the 1,2-diols. The correlation between TOF and diol structure could be rationalized by the fact that mixing of the reactants is increased for diols with a longer chain. In the case of glycerol and ethylene glycol, the substrate is highly polar and the reaction medium remains biphasic for most of the catalytic runs. In the case of diols with longer chains, the polarity difference between the substrate and butadiene/product phases is much smaller and a monophasic system is obtained much faster.

Carbohydrates and sugar alcohols

Carbohydrates are another interesting class of substrates for the telomerization reaction. Sugars, such as glucose (**11**) and xylose (**9**), are easily obtained from the (hemi)cellulose fraction of biomass via hydrolysis. After telomerization, non-ionic surfactant-type molecules are obtained that possess suitable properties for detergent applications. Indeed, the telomerization of glucose (**11**) and sucrose (**17**) has been patented several times [19]. Over the years, much research has been devoted to the selective telomerization of sugars and starch, and a recent review covers many of the different approaches that have been taken for the preparation of octadienyl glycosides [4b]. In the case of telomerization with carbohydrates, the use of solvents is unavoidable owing to the high polarity of these substrates. In contrast to the reactions of glycerol and ethylene glycol, the mono-telomers of sugars are water-soluble and higher substituted products are inevitably obtained also when biphasic conditions are employed. Therefore, in the case of telomerization of carbohydrates, the degree of substitution (**D.S.**) (i.e., the average number of octadienyl chains per substrate) is a more relevant parameter than the mono-telomer selectivity. Since it is expected that the degradation of (hemi)cellulose may yield a variety of different sugars, we decided to screen the activity of Pd/TOMPP with a representative set of carbohydrates that includes examples of all the relevant classes of carbohydrates (Fig. 4) [6d]. Of the aldopentoses we selected D-xylose (**9**) and L-arabinose (**10**) since these are mainly obtained from the depolymerization of hemicellulose. Of the aldohexoses, D-glucose (**11**) was chosen as the main constituent of starch and cellulose. D-mannose (**13**) and D-galactose (**14**) were included for comparison. The ketoses, D-fructose (**15**), and L-sorbose (**16**) were also included as it is known that they may result from the acid- or base-catalyzed isomerization of glucose. Of the disaccharides, D-sucrose (**17**) was selected since it is already produced on a large scale. Finally, cellobiose (**18**) was also included as a model for cellulose.

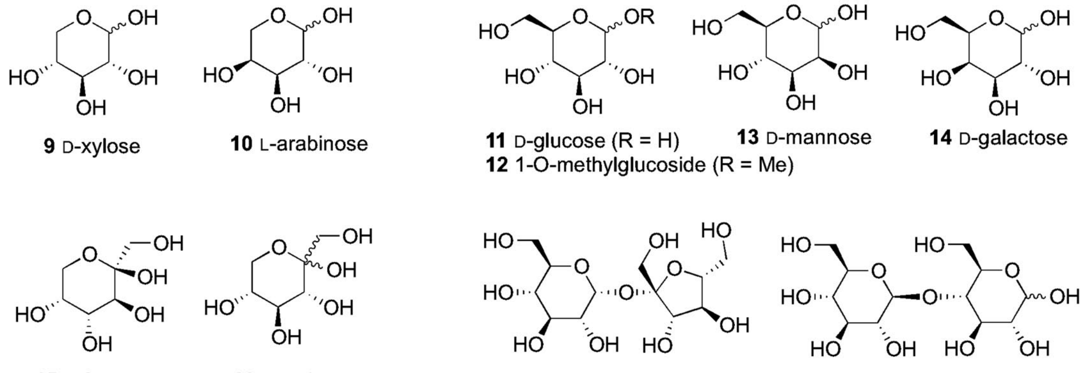

9 D-xylose

10 L-arabinose

11 D-glucose (R = H)

12 1-O-methylglucoside (R = Me)

13 D-mannose

14 D-galactose

15 D-fructose

16 L-sorbose

17 D-sucrose

18 Cellobiose

Fig. 4 Carbohydrates screened in the base-free Pd/TOMPP catalyzed telomerization of 1,3-butadiene [6d].

Preliminary test reactions had shown that DMF (DMF: *N*,*N*-dimethylformamide), which is a commonly used solvent for the telomerization with carbohydrates, leads to low yields in the case of Pd/TOMPP catalysis. In contrast, DMAc (DMAc: *N*,*N*-dimethylacetamide) gave much better yields and was used as a solvent instead. For all reactions, 0.02 mol % Pd(acac)$_2$ with respect to the number of hydroxyl groups was used with a **P/Pd** ratio of 4. For monosaccharides, the **Bu/S** ratio was set at 4, whereas for disaccharides a **Bu/S** ratio of 6 was employed. Reactions were run at 80 °C in a stainless steel autoclave, and the reactor pressure was monitored to study the reaction progression. The results showed that for the aldopentoses (**9**,**10**) and aldohexoses (**11**,**13**,**14**), good substrate conversions (64–95 %) and relatively low **D.S.** values (1.4–2.3) were obtained in all cases. Based on the reactor pressure profiles and the incomplete butadiene conversions (59–82 %), it was also concluded that the catalyst deactivates during the reaction. This was particularly the case for the ketohexoses (**15**,**16**), which displayed even lower butadiene conversions (30–41 %). The disaccharide **17**, in contrast, performed very well and a substrate conversion of 95 % with a butadiene conversion of >97 % was observed (**D.S.** = 3.3). Cellobiose (**18**) on the other hand was unreactive, and a substrate conversion of less than 1 % was found. The poor conversion in case of **18** is explained by the fact that it is very poorly soluble in DMAc. Nevertheless, the deactivation in the case of aldose and ketose sugars appeared to be caused by the participation of the anomeric hydroxyl group, which is absent in the case of **17**. This was confirmed by the reaction of 1-*O*-methylglucoside (**12**), which resulted in 86 % substrate conversion and 95 % butadiene conversion.

Finally, we also included the sugar alcohols glycerol (**1**), *meso*-erythritol (**19**), D-xylitol (**20**) and D-sorbitol (**21**) (Fig. 5) in this screening as they may easily be obtained from sugars by hydrogenation and are already produced on a large scale [20]. A **Bu/S** ratio of 4 was used, and very high substrate conversions (80–93%) and butadiene conversions (94–>97 %) were observed (**D.S.** = 1.8). Also based on the reactor pressure profiles of these reactions, it was found that the reactivity of the substrate correlated with the chain length as the time for full consumption of butadiene decreased considerably going from glycerol (**1**) to sorbitol (**21**).

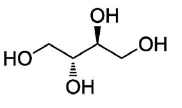
19

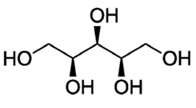
20

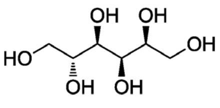
21

Fig. 5 Sugar alcohols screened in the base-free Pd/TOMPP-catalyzed telomerization of 1,3-butadiene [6d].

Deactivation and phosphonium formation

Based on the results discussed above, a clear structure–activity relationship emerged for the Pd/TOMPP-catalyzed telomerization of 1,3-butadiene with biomass-based alcohols (Scheme 3). Substrates that solely possess primary and secondary alcohols (e.g., glycerol, diols, sucrose, and sugar alcohols) gave the best results, and high conversions and selectivities were observed in all cases. The aldoses were somewhat less reactive and resulted in slow deactivation during the catalytic run. The ketoses were the least reactive and resulted in severe deactivation.

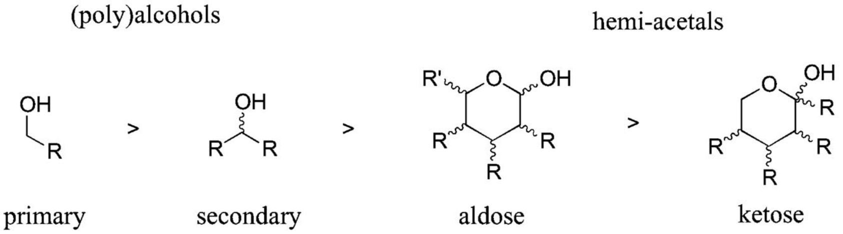

Scheme 3 Reactivity trend observed for biomass-based substrates in the Pd/TOMPP-catalyzed telomerization of 1,3-butadiene [6].

Catalyst deactivation in the case of Pd/PR_3-catalyzed reactions is well known and is generally caused by decomposition of the ligand (e.g., oxidation to phosphine oxides) or the metal (e.g., precipitation to Pd black). To study the observed deactivation in more detail, we analyzed the postcatalytic reaction mixtures using NMR and electrospray ionization-mass spectrometry (ESI-MS). It was found

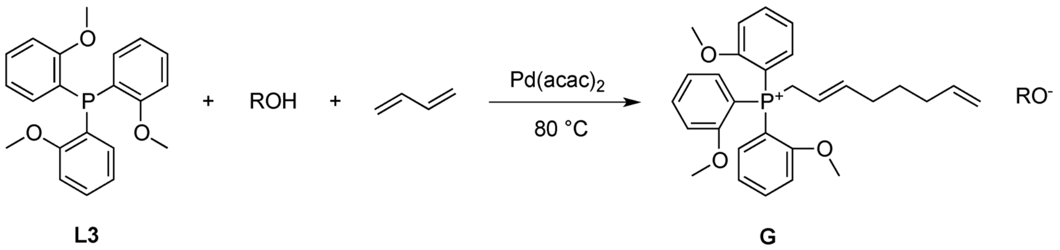

Scheme 4 In situ phosphine alkylation of **L3** to 2,7-octadienylphosphonium alkoxide **G** [8].

that TOMPP (**L3**) is alkylated during the reaction to the corresponding 2,7-octadienylphosphonium derivative (**G**) (Scheme 4) [8].

The amount of **L3** and **G** was quantified for the reaction mixtures of **1**, **20**, **17**, **9**, and **15** (Fig. 6). In cases where no deactivation occurred, the ratio between **L3** and **G** was roughly 1:1, however, in cases where deactivation occurred, the ratio increased to 1>10. This shows that more than 90 % of the ligand is converted during the catalytic run. Since the phosphine is required to stabilize the catalyst, it could be concluded that phosphine depletion was causing the observed deactivation. The formation and even use of ligand-derived phosphonium salts is known in telomerization chemistry and has been reported on several accounts [21]. Most cases, however, deal with the deliberate addition of ligand-derived 2,7-octadienylphosphonium salts to increase catalyst stability. Owing to the strong influence of phosphonium formation on the catalytic activity, we decided to study potential reversibility in more detail.

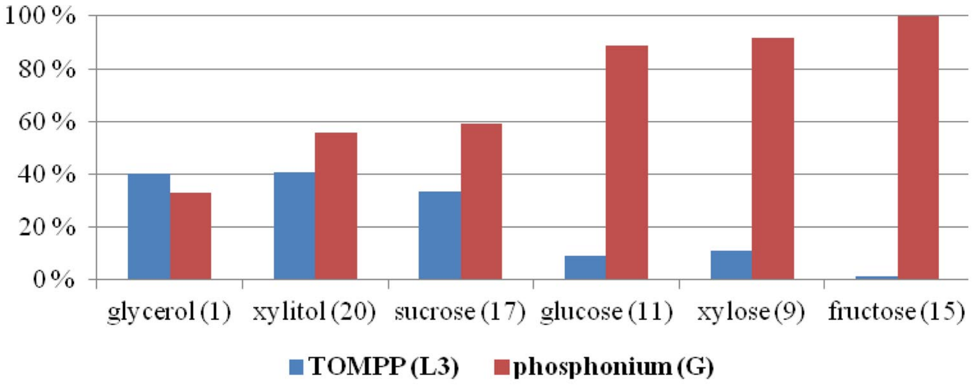

Fig. 6 Postcatalytic ligand composition of the Pd(acac)$_2$/TOMPP-catalyzed telomerization of 1,3-butadiene with carbohydrates and sugar alcohols [8b].

Synthesis of catalytic intermediates

The mechanism of the Pd/PR$_3$-catalyzed telomerization reaction has been studied quite extensively, and most of the relevant catalytic intermediates have been identified and characterized [22]. Particularly, the studies of Jolly et al. [22a,b] and Vollmüller et al. [22c] have contributed to the current understanding of the reaction mechanism (see Scheme 5). As depicted, the overall reaction converts 1,3-butadiene and protic compounds (**NuH**) to linear (**n**) and branched (**iso**) telomers in an atom-efficient manner. The mechanism starts with a postulated zerovalent mono-phosphine, bis-butadiene species [Pd((1,2η)-s-*trans*-buta-1,3-diene)(1,2η)-s-*cis*-buta-1,3-diene)(PR$_3$)] (**A**), which is formed in situ from the precatalyst and ligand. Oxidative coupling of the butadiene ligands yields the bis-allylic species [Pd((1,6-8η)-(*Z*/*E*)-octa-2,6-dien-1,8-diyl)(PR$_3$)] (**B**). In the presence of **NuH**, the σ-allylic fragment of **B** acts as a

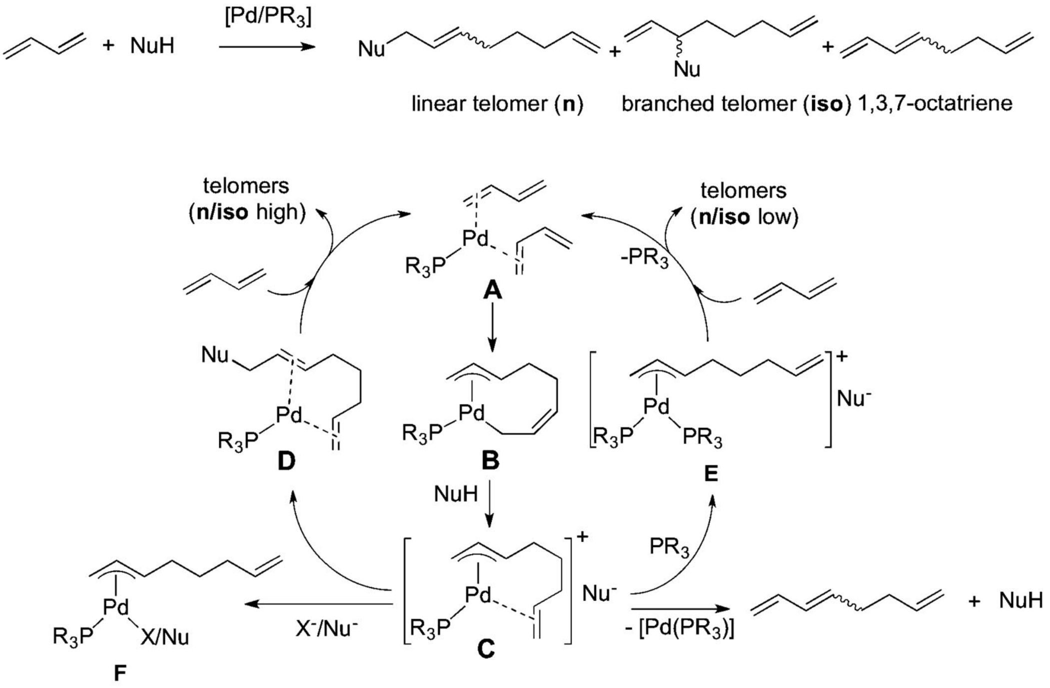

Scheme 5 Overall reaction and generally accepted reaction mechanism of the Pd/PR$_3$-catalyzed telomerization of 1,3-butadiene with NuH.

base and is protonated at the 3-position of the octadiendiyl chain resulting in the ionic complex [Pd((1-3,7,8η)-(*E*)-octa-2,7-dien-1-yl)(PR$_3$)] (**Nu**) (**C**). The 1- and 3-positions of the π-allylic fragment of **C** are susceptible to nucleophilic attack and after reaction with **Nu**$^-$ result in product complexes Pd((2,3,7,8η)-1-**Nu**-(*E*)-octa-2,7-diene)(PR$_3$) (**D**) and Pd((1,2,7,8η)-3-**Nu**-(*E*)-octa-2,7-diene)(PR$_3$) (not shown), respectively. For **C** there is a clear preference for attack at the 1-position and telomers with high **n/iso** ratios are typically observed. After displacement of the ligated telomer by butadiene, **A** is regenerated and the cycle completed. Depending on the ligand-to-metal ratio (**P/Pd**) used in the reaction, it is also possible that the η^2-olefin ligand of **C** is substituted by PR$_3$ resulting in the formation of bis-phosphine complex [Pd((1-3η)-(*E*)-octa-2,7-dien-1-yl)(PR$_3$)$_2$](**Nu**) (**E**). Like **C**, **E** is susceptible to nucleophilic attack of **Nu**$^-$. Owing to different electronic and steric properties, the regioselectivity of attack on **E** is considerably different than that of **C**. For example, stoichiometric reactions have shown that the nucleophilic addition of **Nu**$^-$ to **E** results in much lower n/iso ratios [22c].

It has also been shown that the displacement of the η^2-olefin of **C** by halides (**X**$^-$) or soft nucleophiles may yield the neutral complex [Pd**X**((1-3η)-(*E*)-octa-2,7-dien-1-yl)(PR$_3$)] (**F**), which is supposedly less reactive and may therefore lead to suppression of the catalytic activity or even complete deactivation. This is in line with the observation that Pd(II) precatalysts, which contain halide ligands, are inactive as discussed above. The formation of by-products such as 1,3,7-octatriene is also commonly observed and is considered to proceed via a formal proton abstraction from complex **C**. As discussed above, it has also been shown that the formation of ligand-derived phosphonium species may occur and that this process has a strong influence on the catalytic activity [8b,21]. Taking into account that TOMPP is a good nucleophile owing to the strong electron-donating effect of the *ortho*-methoxy substituents, it is obvious that phosphonium **G** is formed from the nucleophilic addition of TOMPP to **C**. Given the reported use of **G** as a ligand reservoir, we decided to study the reversibility of the observed reaction [21]. Stoichiometric coordination reactions were performed using Pd(dba)$_2$ and tris(2-

methoxyphenyl((*E*)-octa-2,7-dien-1-yl)phosphonium iodide (**22**) and resulted in the formation of the neutral complex [PdI((1-3η)-(*E*)-octa-2,7-dien-1-yl)(TOMPP)] (**23**) (Scheme 6) [8b]. The crystal structure of **23** was determined by X-ray crystallography and constitutes the first example of a complex of type **F** (Fig. 7, left). Based on these results, it could be concluded that the oxidative addition of **22** occurs in the presence of Pd(0).

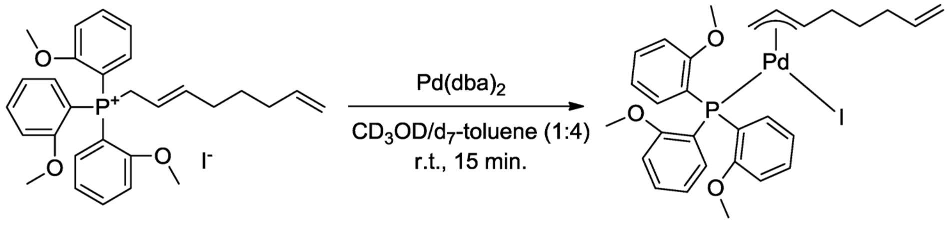

22

23 (74 %)

Scheme 6 Stoichiometric coordination reaction of tris(2-methoxphenyl)((*E*)-octa-2,7-dien-1-yl) phosphonium iodide (**22**) with Pd(dba)$_2$ resulting in [PdI((1-3η)-(*E*)-octa-2,7-dien-1-yl)(TOMPP)] (**23**) [8].

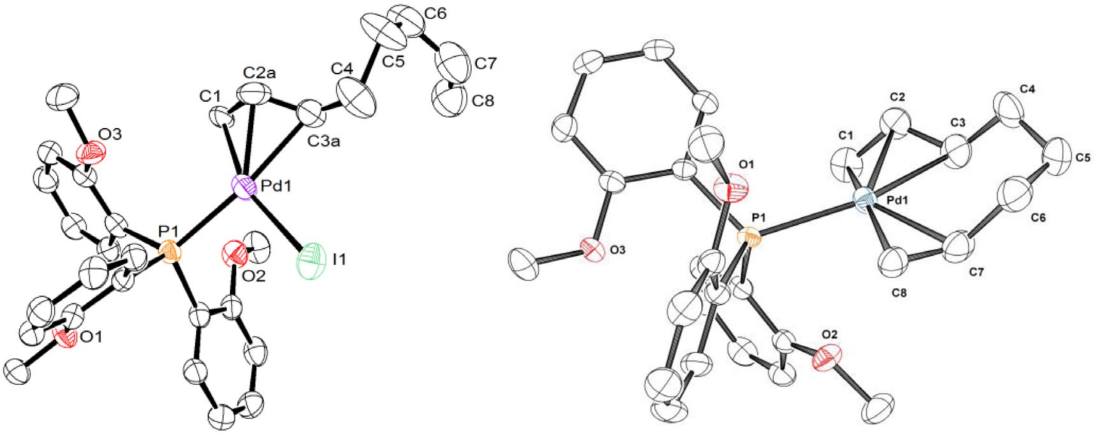

Fig. 7 ORTEP diagrams of the X-ray crystal structures of [PdI((1-3η)-(*E*)-octa-2,7-dien-1yl)(TOMPP)] (**23**, left) and [Pd((1-3,7,8η)-(*E*)-octa-2,7-dien-1-yl)(TOMPP)] BF$_4$ (**25**, right). Ellipsoids are drawn at 50 % probability. Hydrogen atoms and tetrafluoroborate anion have been omitted for clarity [8].

To rule out the possible involvement of the iodide anion, the same reaction was attempted with tris(2-methoxyphenyl)((*E*)-octa-2,7-dien-1-yl)phosphonium tetrafluoroborate (**24**), which contains the non-nucleophilic and weakly coordinating tetrafluoroborate anion. Surprisingly, no reaction occurred and attempts to enable the reaction by heating failed. Only when a catalytic amount (5 mol %) of TOMPP was added, did the reaction proceed (Scheme 7). The reaction was monitored by NMR, and it was found that **24** was directly converted to [Pd((1-3,7,8η)-(*E*)-octa-2,7-dien-1-yl)(TOMPP)] BF$_4$ (**25**), which reached an equilibrium of approximately 1:1 between **24** and **25**. Since **25** is a complex of type **C** (Scheme 9), these results clearly demonstrate that the formation of phosphonium **G** is indeed reversible in the case of Pd/TOMPP.

The equilibrium of 1:1 between **24** and **25** roughly corresponds to the post-catalytic composition of **L3** and **G** observed for substrates for which no catalyst deactivation is observed (Fig. 6). In contrast, for substrates that do lead to catalyst deactivation this equilibrium is considerably shifted toward phosphonium species **G**. Although it is unclear which property of the substrate is causing this shift, it seems

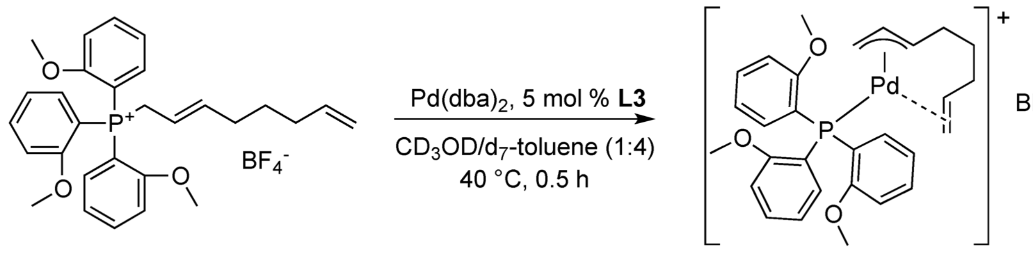

24

25 (50 %)

Scheme 7 Stoichiometric coordination reaction of tris(2-methoxyphenyl)((*E*)-octa-2,7-dien-1-yl)phosphonium tetrafluoroborate with $Pd(dba)_2$ and 5 mol % TOMPP resulting in [Pd((1,3,7,8η)-(*E*)-octa-2,7-dien-1-yl)(TOMPP)] BF_4 (**25**) [8].

likely that the enhanced acidity and reduced nucleophilicity of the hemi-acetal group both contribute to the observed behavior. Also noteworthy is that for these catalytic reactions, $Pd(acac)_2$ was used as precatalyst. Since it is known that the reaction is catalyzed by Pd(0) species, it is possible that in the initial stage of the reaction, the formation of phosphonium **G** proceeds much faster than the reduction of $Pd(acac)_2$. As such, **G** cannot reenter the cycle, owing to the incompatibility with $Pd(acac)_2$, and the reaction deactivates as a result of phosphine depletion. Therefore, these reactions were repeated with $Pd(dba)_2$ as precatalyst and resulted, in the case of xylose (**9**) and glucose (**11**), in markedly improved activities. Nevertheless, for fructose (**15**) severe deactivation was still observed.

In analogy to the reversibility of phosphonium formation, we also studied the reversibility of the product formation reaction (Scheme 5, **D** to **C**) [8]. The results of Kuntz et al. already showed that for Pd/TPPTS oxidative addition of allylic alcohols occurs in a wide pH range and results in the formation of π-allyl complexes with liberation of OH^- [21f,g]. Thus, if 1 equiv of acid is added to the reaction, the equilibrium can be steered toward complete conversion to the π-allyl complex. With this in mind, a simple one-pot procedure was developed that allows efficient synthesis of complexes of type **C** (Scheme 8). To a solution of $Pd(dba)_2$ and 2 equiv 2,7-octadienol in CH_2Cl_2, 1 equiv of triarylphosphonium tetrafluoroborate salt ($[HPR_3]BF_4$: **27**, R = Ph; **28**, R = 4-MeOPh; **29**, R = 2-MeOPh; **30**, R = 2-MePh) was slowly added dropwise, which resulted in high isolated yields of the corresponding $[Pd((1,3,7,8\eta)$-(*E*)-octa-2,7-dien-1-yl)$(PR_3)]BF_4$ complexes **31** (91 %): R = Ph [21c]; **32** (78 %): R = 4-MeOPh; **25** (88 %): R = 2-MeOPh; **33** (94 %): R = 2-MePh). The structures of **31** [21c] and **25** (Fig. 7, right) were determined by X-ray crystallography and confirm the η^3,η^2 bonding mode of the octadienyl ligand. These structures represent the first structural characterization of complexes of type **C**.

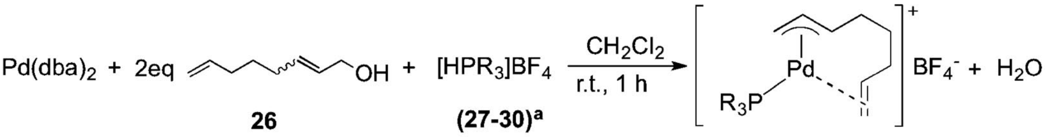

26 **(27-30)**[a] **(31,32,25,33)**[a]

Scheme 8 One-pot synthesis of $[Pd((1,3,7,8\eta)$-(*E*)-octa-2,7-dien-1-yl)$(PR_3)]BF_4$ complexes. (a) **27**, **31** (91 %): R = Ph [21c]; **28**, **32** (78 %): R = 4-MeOPh; **29**, **25** (88 %): R = 2-MeOPh; **30**, **33** (94 %): R = 2-MePh [8].

The same procedure was also attempted for TPPTS (**L9**), however, synthesis of the corresponding phosphonium tetrafluoroborate salt is complicated owing to the sulfonate groups. Instead, the procedure was modified by introducing 3 equiv HBF_4 to the reaction mixture before the addition of the ligand. Owing to the poor solubility of the ligand in CH_2Cl_2, a 1:1 CH_2Cl_2/MeOH mixture was used to improve solubility (Scheme 9). The reaction was performed and after work-up by precipitation from MeOH/acetone, 85 % of $Na_2[Pd((1,3,7,8\eta)$-(*E*)-octa-2,7-dien-1-yl)(TPPTS)] (**34**) was obtained. These results show that this reaction is generally applicable to a wide range of phosphines and demonstrates that the product formation reaction (Scheme 5, **D** to **C**) can be reversed under the influence of stoichiometric amounts of acid.

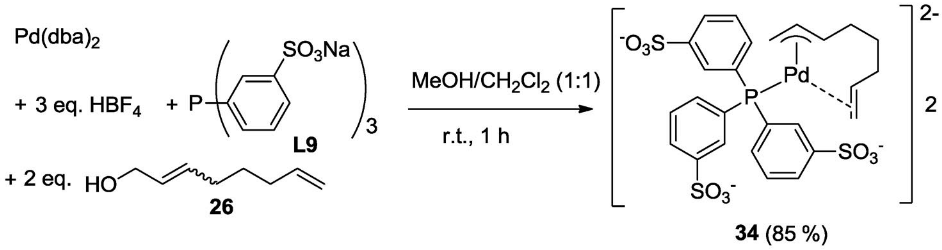

Scheme 9 One-pot synthesis of $Na_2[Pd((1,3,7,8\eta)$-(*E*)-octa-2,7-dien-1-yl)(TPPTS)] (**34**) [8].

To study the influence of the ligand backbone on the reactivity of complexes **C**, we have performed stoichiometric nucleophilic addition reactions of sodium methoxide on complexes **25**, **31**, **32**, **33**, and **34**. Reactions were performed in methanol at room temperature and the progress of the reaction was monitored using UV–vis. In all cases, the spectra showed that a band at 310–316 nm decreased in intensity upon addition of sodium methoxide. From this data initial rates were extrapolated and reported relative to the reaction rate of PPh_3 complex **31** (Scheme 10). The rates were compared to parameters such as the Tolman cone angle (θ (°)) and the carbonyl stretch (ν_{CO} (cm^{-1})) of the corresponding $Ni(CO)_3(PR_3)$ complexes, however, no clear correlation could be discovered. Rather, the empirical reactivity trend could be rationalized from a combination of steric, electronic, and electrostatic considerations.

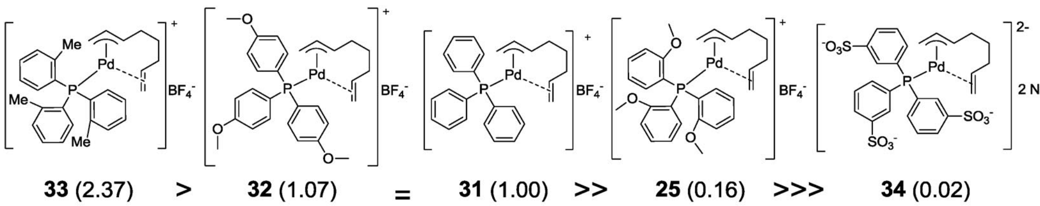

Scheme 10 Reactivity trend and relative rates observed for complexes **25**, **31**, **32**, **33**, and **34** in the stoichiometric nucleophilic addition reaction with NaOMe [8].

Variable-temperature NMR revealed that complex **33** is in dynamic exchange between various structural isomers owing to the rather large cone angle (194°) of **L6**. Based on this, it was concluded that the increased rate of **33** can be attributed to a destabilization of the complex caused by steric interactions between the ligand and the metal fragment. Complex **32** displayed an approximately equal rate as **31** and shows that increased electron donation of **L8** only has a small effect on the reactivity of the complex. Surprisingly, the rate of complex **25** is considerably slower than that of **31**. Although **L3** possesses a rather large cone angle (176°), variable-temperature NMR showed that the steric interaction of the ligand with the metal fragment is much less than in case of **33**. The decreased reactivity of **25** was attributed to a combination of strong electron donation and electrostatic or hemi-labile interaction of the *ortho*-methoxy substitutents. Both properties result in a good distribution of the cationic charge over the ligand and as such reduces the reactivity of complex. This is particularly the case for TPPTS complex **34**, where the trianionic ligand compensates the cationic charge of the metal fragment. As a result, the approach of the methoxide anion is unfavorable and a severely decreased rate is observed. This is well in line with the fact that Pd/TPPTS-catalyzed reactions generally require the addition of a base to enhance the catalytic performance. In relation to catalytic results, it appears that decreased reactivity and hence increased stability of complex **C** is more favorable as the highest turnover numbers (TONs) are typically observed for ligands such as PPh_3, **L3**, and **L9**.

Based on these studies, we proposed an extension to the generally accepted telomerization mechanism which accounts for the in situ formation of phosphonium **G** and the reversibility of reaction pathways (Scheme 11). As shown, the reaction of PR_3 with complex **C** can result either in the formation of **E**, or (via complex **D(P⁺)**) in phosphonium **G**. Following this reasoning, the counterion of **G** has to be **Nu⁻**. Thus, the formation of **G** effectively raises the concentration of **Nu⁻** with respect to **C**. This may explain why, in the case of Pd/TOMPP, catalysis proceeds swiftly without the use of an added base. Stoichiometric coordination reactions confirm that this reaction is fully reversible in the presence of Pd(0) and catalytic amounts of ligand (Schemes 6 and 7). Therefore, in the case of Pd/TOMPP, **G** acts as a ligand reservoir and controls the course of the reaction via reversible formation of complex **C** and increasing the concentration of **Nu⁻** [21]. The relevance of this route will strongly depend on which catalyst system is employed, and it is expected that particularly phosphines that result in stable complexes **C** (e.g., Pd/TOMPP and Pd/TPPTS) also give rise to **G**. Besides this, the synthesis of complexes **C** from 2,7-octadienol (**26**) also demonstrates that the product formation route (**C** to **D**) is reversible and is mainly influenced by the pH of the reaction mixture (Scheme 11).

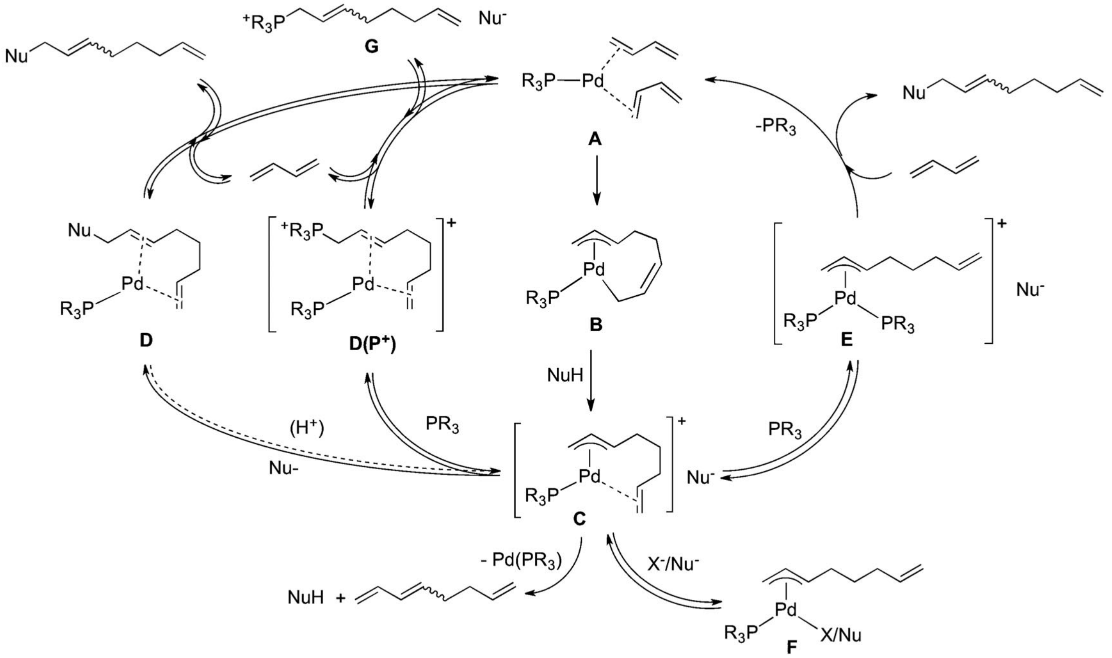

Scheme 11 Extended mechanism for Pd/TOMPP-catalyzed telomerization of 1,3-butadiene with NuH [8].

CONCLUSIONS

A ligand screening was performed for the Pd-catalyzed telomerization of 1,3-butadiene with glycerol, and the results showed that TOMPP provides the most active catalyst of the investigated series. Optimization of reaction conditions was performed and resulted in a solvent- and base-free protocol that could also be successfully applied to crude glycerol. A set of linear and branched diols was tested under the same conditions and high yields, and good selectivities toward the mono-telomer were observed in all cases. It was found that the structure of the diol correlates to the initial TOF of the reaction and TOFs of up to 400 000 h^{-1} were observed. A representative selection of carbohydrates and sugar alcohols were screened, and high conversions and relatively low degrees of substitution were observed for most of the studied substrates. A clear structure–activity relationship was observed, which shows that primary and secondary hydroxyl groups are most reactive. Only in the case of hemi-acetal-bearing sugars, deactivation of the catalyst was observed. These results clearly demonstrate that Pd/TOMPP is a highly active catalyst for the telomerization of 1,3-butadiene with biomass-based polyols. Mechanistic studies were performed and showed that the hemi-acetal-induced catalyst deactivation is related to extensive formation of ligand-derived phosphonium species. Stoichiometric coordination reactions prove the reversibility of reaction pathways and allowed efficient synthesis of catalytic intermediates. The first examples of crystal structures of intermediates **C** and **F** were obtained. Based on these studies, an extended telomerization mechanism is proposed, which accounts for the formation of ligand-derived phosphonium species and the reversibility of reaction pathways. Finally, the presented studies demonstrate that the interplay between catalysis and organometallic synthesis provides useful insights and allows detailed mechanistic studies to be performed.

REFERENCES

1. A. Corma, S. Iborra, A. Velty. *Chem. Rev*. **107**, 2411 (2007).
2. J. Zakzeski, P. C. A. Bruijnincx, A. L. Jongerius, B. M. Weckhuysen. *Chem. Rev.* **110**, 3552 (2010).
3. (a) J. A. Melero, G. Vicente, G. Morales, M. Paniagua, J. M. Moreno, R. Roldán, A. Ezguerro, G. Pérez. *Appl. Catal., A* **346**, 44 (2008); (b) C. Klepáčová, D. Mravec, M. Bajus. *Appl. Catal., A* **294**, 141 (2005); (c) C. Klepáčová, D. Mravec, A. Kaszonyi, M. Bajus. *Appl. Catal., A* **328**, 1 (2007); (d) R. S. Karinen, A. O. I. Krause. *Appl. Catal., A* **306**, 128 (2006); (e) A. Behr, L. Obendorf. *Chem.-Ing.-Tech.* **73**, 1463 (2001); (f) A. Behr, J. Eilting, K. Irawadi, J. Leschinki, F. Lindner. *Green Chem.* **10**, 13 (2008).
4. (a) A. Behr, M. Becker, T. Beckmann, L. Johnen, J. Leschinski, S. Reyer. *Angew. Chem., Int. Ed.* **48**, 3598 (2009); (b) S. Bouquillon, J. Muzart, C. Pinel, F. Rataboul. *Top. Curr. Chem.* **295**, 93 (2010).
5. (a) A. M. Ruppert, A. N. Parvulescu, M. Arias, P. J. C. Hausoul, P. C. A. Bruijnincx, R. J. M. Klein Gebbink, B. M. Weckhuysen. *J. Catal.* **268**, 251 (2009); (b) A. N. Parvulescu, D. Mores, E. Stavitski, C. M. Teodorescu, P. C. A. Bruijnincx, R. J. M. Klein Gebbink, B. M. Weckhuysen. *J. Am. Chem. Soc.* **132**, 10429 (2010).
6. (a) R. Palkovits, I. Nieddu, R. J. M. Klein Gebbink, B. M. Weckhuysen. *ChemSusChem* **1**, 193 (2008); (b) R. Palkovits, I. Nieddu, C. A. Kruithof, R. J. M. Klein Gebbink, B. M. Weckhuysen. *Chem.—Eur. J.* **14**, 8995 (2008); (c) R. Palkovits, A. N. Parvulescu, P. J. C. Hausoul, C. A. Kruithof, R. J. M. Klein Gebbink, B. M. Weckhuysen. *Green Chem.* **11**, 1155 (2009); (d) P. J. C. Hausoul, P. C. A. Bruijnincx, R. J. M. Klein Gebbink, B. M. Weckhuysen. *ChemSusChem* **2**, 855 (2009).
7. A. N. Parvulescu, P. J. C. Hausoul, P. C. A. Bruijnincx, R. J. M. Klein Gebbink, B. M. Weckhuysen. *Catal. Today* **158**, 130 (2010).
8. (a) P. J. C. Hausoul, A. N. Parvulescu, M. Lutz, A. L. Spek, P. C. A. Bruijnincx, B. M. Weckhuysen, R. J. M. Klein Gebbink. *Angew. Chem., Int. Ed.* **49**, 7972 (2010); (b) P. J. C. Hausoul, A. N. Parvulescu, M. Lutz, A. L. Spek, P. C. A. Bruijnincx, R. J. M. Klein Gebbink, B. M. Weckhuysen. *ChemCatChem* **3**, 845 (2011).
9. Y. Tokitoh, T. Higashi, K. Hino, M. Murasawa, N. Yoshimura (Kuraray). U.S. Patent 5118885 (1992).

10. (a) J. Briggs, J. Patton, S. Vermaire-Louw, P. Margl, H. Hagen, D. Beigzadeh. (Dow Global Technologies, Inc.). WO 2010019360 (2010); (b) P. Van Leeuwen, M. Tschan, E. J. Garcia-Suarez, Z. Freixa, H. Hagen, (DOW). WO 2010120846 A2 (2010).
11. J. A. Kenar. *Lipid Tech.* **19**, 249 (2007).
12. (a) A. Behr, M. Urschey. *Adv. Synth. Catal.* **345**, 1242 (2003); (b) A. Behr, J. Leschinski, C. Awungacha, S. Simic, T. Knoth. *ChemSusChem* **2**, 71 (2009).
13. T. Prinz, B. Driessen-Hölscher. *Chem.—Eur. J.* **5**, 206 (1999).
14. B. Estrine, S. Bouquillon, F. Hénin, J. Muzart. *Eur. J. Org. Chem.* 2914 (2004).
15. (a) M. J.-L. Tschan, E. J. Garcia-Suarez, Z. Freixa, H. Launay, H. Hagen, J. Benet-Buchholz, P. W. N. M. van Leeuwen. *J. Am. Chem. Soc.* **132**, 6463 (2010); (b) M. J.-L. Tschan, J.-M. Lopez-Valbuena, Z. Freixa, H. Launay, H. Hagen, J. Benet-Buchholz, P. W. N. M. van Leeuwen. *Organometallics* **30**, 792 (2011); (c) J. R. Briggs, H. Hagen, J. Samir, J. T. Patton. *J. Organomet. Chem.* **696**, 1677 (2011).
16. (a) H. Fukutani, M. Tokizawa, Y. Nishikawa, H. Okada, (Mitsubishi). JP 48039413 (1973); (b) K. Matsuzaki, R. Tsumura, T. Sakamoto, (Mitsui). JP 49031965 (1974); (c) S. Enomoto, Y. Ohmura, H. Wada, Y. Mukaida, M. Yanaka, H. Takita, (Kureha). JP 51142532 (1976).
17. (a) H. S. Broadbent, G. C. Campbell, W. J. Bartley, J. H. Johnson. *J. Org. Chem.* **24**, 1847 (1959); (b) T. C. Forschner, J. B. Powell, L. H. Slaugh, P. R. Weider. WO 2000/018712 (2000); (c) U. Herrmann, G. Emig. *Ind. Eng. Chem. Res.* **36**, 2885 (1997); (d) N. S. Dunn-Coleman, M. Diaz-Torres, M. W. Chase, D. Trimbur. WO 98/21341 (1998); (e) J. van Haveren, E. L. Scott, J. Sanders. *Biofuels, Bioprod. Bioref.* **2**, 41 (2008).
18. (a) U. M. Dzhemilev, R. V. Kunakova, N. Z. Baibulatova, G. A. Tolstikov, A. A. Panasenko. *Zh. Org. Khim.* **16**, 1157 (1980); (b) K. Kaneda, H. Kurosaki, M. Terasawa, T. Imanaka, S. Teranishi. *J. Org. Chem.* **46**, 2356 (1981); (c) A. Behr, M. Urshey. *J. Mol. Catal., A* **197**, 101 (2003); (d) A. Behr, M. Urshey, V. A. Brehme. *Green Chem.* **5**, 198 (2003).
19. (a) B. Gruber, K. J. Weese, H. P. Mueller, K. Hill, A. Behr, J. R. Tucker, S. M. Hoagland, (Henkel). WO 92/01702 (1992); (b) K. Hill, K. J. Weese. DE 4242467 (1993); (c) I. Pennequin, A. Mortreux, F. Petit, J. Mentech, B. Thiriet. FR 19940107 (Eridania Beghin Say) Brev. Fr. (1994).
20. I. Pennequin, A. Mortreux, F. Petit, J. Mentech, B. Thiriet. FR 2693188 (1994).
21. (a) S. M. Maddock, M. G. Finn. *Organometallics* **19**, 2684 (2000); (b) M. Toshihiko, T. Yasuo, Y. Noraiki. EP 296550 (1988); (c) Y. Kazuyuki, S. Kenji, M. Masahiro, F. Junichi, S. Shigeaki. EP 1249455 (2002); (d) Y. Kazuyuki, S. Shigeaki. JP 2002371090 (2002); (e) A. Behr, J. Leschinski, A. Prinz, M. Stoffers. *Chem. Eng. Process* **48**, 1140 (2009); (f) J.-M. Basset, D. Bouchu, G. Godard, I. Karamé, E. Kuntz, F. Lefebvre, N. Legagneux, C. Lucas, D. Michelet, J. B. Tommasino. *Organometallics* **27**, 4300 (2008); (g) E. Kuntz, J.-M. Basset, D. Bouchu, G. Godard, F. Lefebvre, N. Legagneux, C. Lucas, D. Michelet. *Organometallics* **29**, 523 (2010).
22. (a) R. Benn, P. W. Jolly, R. Mynott, B. Raspel, G. Schenker, K. P. Schick, G. Schroth. *Organometallics* **4**, 1945 (1985); (b) P. W. Jolly, R. Mynott, B. Raspel, K. P. Schick. *Organometallics* **5**, 473 (1986); (c) F. Vollmüller, J. Krause, S. Klein, W. Mägerlein, M. Beller. *Eur. J. Inorg. Chem.* 1825 (2000).